Signal-to-Noise-Ratio Analysis of Compressive Data Acquisition

Pribic, Radmila; Leus, Geert; Tzotzadinis, C.

DOI
10.1109/SSP.2018.8450796

Publication date
2018

Document Version
Final published version

Published in
2018 IEEE Statistical Signal Processing Workshop, SSP 2018

SIGNAL-TO-NOISE-RATIO ANALYSIS OF COMPRESSIVE DATA ACQUISITION

*Radmila Pribić** *Geert Leus †* *Christos Tzotzadinis†*

*Sensors Advanced Developments, Thales Nederland, Delft, The Netherlands

†Delft University of Technology, Delft, The Netherlands

ABSTRACT

Data acquisition in compressive sensing (CS) is commonly believed to be less complicated, and even less costly, while performing agreeably. There is a major lack of measureable foundations supporting this optimism as the performance and complexity of a CS sensor have hardly been quantified. We aim to fill the gap by computing the performance of diverse compressive data acquisition schemes by the output signal-to-noise ratio (SNR) they provide with the same input signal. The SNR is assessed analytically, and also confirmed numerically with simulated data. Only with a scheme of compressive data acquisition starting directly at reception (with no receiver noise yet), CS is less complicated and still performs as good as, if not better than, existing sensing.

Index Terms— compressive sensing, data acquisition, signal-to-noise ratio, performance

1. INTRODUCTION

Compressive sensing (CS) is a recent paradigm in sensing that works with a reduced number of measurements for a comparable sensing result. This is possible because CS is optimized to available information in measurements rather than to the sensing bandwidth only. The optimization is based on two conditions: sparsity of sensing results and the sensing incoherence (e.g. [1]). In a CS sensor, sparse signal processing (SSP) is crucial in the back end, while its front end facilitates compressive data acquisition. The ultimate goal of CS is to create a CS sensor which can be less complicated and still can perform at least as good as, or preferably even better, than existing sensors.

Compressive data acquisition is regularly believed to be less complicated (and even less costly) while performing satisfactorily (e.g. [2]-[5]). However, there are no exact grounds provided for this optimism as the performance and complexity have almost never been quantified.

The performance and overall processing gain in CS are becoming additionally important and delicate due to fewer measurements (e.g. [6]-[7]). As we focus on a CS sensor as a whole, we check how fewer measurements from the compressive data acquisition affect the performance of SSP in the back end. Therefore, we measure the performance of different compressive data acquisition schemes by their output signal-to-noise ratio (SNR) given the same input signal. We show that only with compressive data acquisition directly at reception (e.g. [8] and [9]), the front end with CS simplifies while performing as good as existing sensors.

1.1. Related Work

Compressive data acquisition was much investigated in the last decade and commonly anticipated to be better (e.g. [2]-[5]). There is a substantial lack of concrete quantities underlying this assertion. Recently in [9], we started investigating the balance between the performance and complexity of typical front-end architectures in CS. In this paper, we focus on the performance given by the output SNR.

1.2. Outline and Main Contributions

In Section 2, relevant data acquisition schemes are presented starting with the Nyquist-sampled scheme as the reference, followed by typical sub-Nyquist schemes with compression before, at and after reception. In Section 3, their performance is analyzed by the output SNR. In Section 4, numerical results are presented. In Section 5, conclusions are drawn and future work is indicated. In Section 6, details of the performance analysis are given in an appendix.

Our main contributions are the performance analysis of different data acquisition schemes in CS. Furthermore, we compare compressive data acquisition with a corresponding existing scheme as the reference. Finally, we look at a CS sensor as a whole. We reveal that a CS sensor with certain compressive data acquisition can be less involved and still perform as good as, if not better than, existing sensors.

2. COMPRESSIVE DATA ACQUISITION

Compressive data acquisition may change processing gain and sensing performance (e.g. [6]-[7]). We are interested in data acquisition schemes with Nyquist-sampled data as the reference, and typical sub-Nyquist data acquisition schemes with compression before, at and after reception.

Raw complex-valued measurements gathered in a vector $\boldsymbol{y} \in \mathbb{C}^N$ of an input (true) signal $\boldsymbol{s}$ can be modeled as:

$$\boldsymbol{y} = \boldsymbol{A}_t \boldsymbol{s} + \boldsymbol{z}\,, \tag{1}$$

where $\boldsymbol{A}_t \in \mathbb{C}^{N\text{x}K}$ is a sensing matrix at $\boldsymbol{s} \in \mathbb{C}^K$ and $\boldsymbol{z} \in \mathbb{C}^N$ is a (complex Gaussian) receiver-noise vector of i.i.d. elements with zero mean and equal variances γ, $\boldsymbol{z} \sim CN(\boldsymbol{0}, \gamma \boldsymbol{I}_N)$.

2.1 Nyquist-sampled scheme

For the sake of simplicity, we investigate the CS performance when $\boldsymbol{s}$ contains a single nonrandom component only, i.e.

978-1-5386-1570-3/18/$31.00 ©2018 IEEE

when K =1. Accordingly, the reference Nyquist-sampled (NS) data $\boldsymbol{y} \in \mathbb{C}^{Nx1}$ can be written as:

$$\boldsymbol{y} = \boldsymbol{a}s + \boldsymbol{z} \tag{2}$$

where $\boldsymbol{a} \in \mathbb{C}^{Nx1}$ is a column of $\boldsymbol{A}_t$ belonging to the nonzero response s and $\boldsymbol{z}$ is as before, $\boldsymbol{z} \sim CN(\boldsymbol{0}, \gamma \boldsymbol{I}_N)$. The sensing vector $\boldsymbol{a}$ is nonrandom and exponential (as e.g. in DOA) with norm $\sqrt{N}$, $\|\boldsymbol{a}\| = \sqrt{N}$ as $|a_n| = 1$, $n = 1, \ldots, N$.

2.2 Sub-Nyquist schemes

We investigate compressive data acquisition with three typical sub-Nyquist data models. First we look at models related to compression before and after reception, namely to sparse sensing (SS, e.g. [4]) and analog-to-information conversion (AIC, e.g. [2], [3] and [5]), respectively. Further, we look at a recent scheme of random mask (RM, e.g. [8] and [9]) which enables the compression directly at reception.

In the SS and AIC cases, the model of compressed data $\boldsymbol{y}_{\mathrm{c}} \in \mathbb{C}^M$ (c being ss or aic), $M < N$, can be written as follows:

$$\boldsymbol{y}_{\mathrm{c}} = \boldsymbol{B}_{\mathrm{c}}\boldsymbol{y} = \boldsymbol{B}_{\mathrm{c}}\boldsymbol{a}s + \boldsymbol{B}_{\mathrm{c}}\boldsymbol{z} = \boldsymbol{a}_{\mathrm{c}}s + \boldsymbol{z}_{\mathrm{c}} \tag{3}$$

where $\boldsymbol{B}_{\mathrm{c}}$ is a compression matrix, $\boldsymbol{B}_{\mathbf{c}} \in \mathbb{C}^{MxN}$.

In the SS case, $\boldsymbol{B}_{\mathrm{ss}}$ has M ones (chosen in a multi-coset manner, e.g. [4]) one on every row and zeros elsewhere. Accordingly, $\boldsymbol{y}_{\mathrm{ss}}$, $\boldsymbol{a}_{\mathrm{ss}}$ and $\boldsymbol{z}_{\mathrm{ss}}$ contain the corresponding M elements from $\boldsymbol{y}$, $\boldsymbol{a}$ and $\boldsymbol{z}$, respectively. Thus, there are M outputs, each output having the noise corresponding to the noise in the reference case, $\boldsymbol{z}_{\mathrm{ss}} \sim CN(\boldsymbol{0}, \gamma \boldsymbol{I}_M)$. The noise $\boldsymbol{z}_{\mathrm{ss}}$ remains white because $\boldsymbol{B}_{\mathrm{ss}}\boldsymbol{B}_{\mathrm{ss}}^{\mathrm{H}}$ equals $\boldsymbol{I}_M$.

In AIC, $\boldsymbol{B}_{\mathrm{aic}}$ is a full random matrix. We investigate a practical $\boldsymbol{B}_{\mathrm{aic}}$ which contains uniformly-distributed phase shifts. Accordingly, $\boldsymbol{y}_{\mathrm{aic}}$, $\boldsymbol{a}_{\mathrm{aic}}$ and $\boldsymbol{z}_{\mathrm{aic}}$ are the result of the projection of $\boldsymbol{y}$, $\boldsymbol{a}$ and $\boldsymbol{z}$, respectively, with $\boldsymbol{B}_{\mathrm{aic}}$. If $\boldsymbol{B}_{\mathrm{aic}}$ would be a single realization (and thus, could be treated as nonrandom), $\boldsymbol{z}_{\mathrm{aic}} \sim CN\left(\boldsymbol{0}, \gamma \boldsymbol{B}_{\mathrm{aic}}\boldsymbol{B}_{\mathrm{aic}}^{\mathrm{H}}\right)$. Otherwise, $\boldsymbol{z}_{\mathrm{aic}}$ is not Gaussian anymore as a product of the uniform $\boldsymbol{B}_{\mathrm{aic}}$ and the Gaussian $\boldsymbol{z}$. The noise $\boldsymbol{z}_{\mathrm{aic}}$ might also not be white anymore because $\boldsymbol{B}_{\mathrm{aic}}\boldsymbol{B}_{\mathrm{aic}}^{\mathrm{H}}$ could deviate from the identity matrix.

In the RM case, the related model of compressed data $\boldsymbol{y}_{\mathrm{rm}} \in \mathbb{C}^M$, $M < N$, can be written as follows:

$$\boldsymbol{y}_{\mathrm{rm}} = \boldsymbol{B}_{\mathrm{rm}}\boldsymbol{a}s + \boldsymbol{z}_{\mathrm{rm}} = \boldsymbol{a}_{\mathrm{rm}}s + \boldsymbol{z}_{\mathrm{rm}} \tag{4}$$

where $\boldsymbol{B}_{\mathrm{rm}}$ is a compression matrix. For the sake of a clear comparison, we assume the same random compression matrix $\boldsymbol{B}$ in both RM and AIC cases, $\boldsymbol{B} = \boldsymbol{B}_{\mathrm{rm}} = \boldsymbol{B}_{\mathrm{aic}}$. In RM, $\boldsymbol{B}_{\mathrm{rm}}$ affects only the signal as it works at reception without any receiver noise yet. After reception there are M outputs whose receiver noise is equivalent to the SS case, i.e. $\boldsymbol{z}_{\mathrm{rm}} \sim CN(\boldsymbol{0}, \gamma \boldsymbol{I}_M)$. In AIC, $\boldsymbol{B}_{\mathrm{aic}}$ affects both the signal and receiver noise as it occurs after reception in a CS sensor.

In CS, the solution for the unknown s from data models (2)-(4) is sought by applying the model: $\boldsymbol{y}_{\mathrm{c}} = \boldsymbol{A}_{\mathrm{c}}\boldsymbol{x} + \boldsymbol{z}_{\mathrm{c}}$ where $\boldsymbol{A}_{\mathrm{c}}$ is the sensing matrix over a discrete grid of size N, $\boldsymbol{A}_{\mathrm{c}} \in \mathbb{C}^{MxN}$ and $\boldsymbol{x}$ is a sparse vector, $\boldsymbol{x} \in \mathbb{C}^N$. The usual sparse signal processing (SSP), e.g. LASSO [10], applies as:

$$\boldsymbol{x}_{\mathrm{SSP}} = \arg\min_{\boldsymbol{x}} \|\boldsymbol{y}_{\mathrm{c}} - \boldsymbol{A}_{\mathrm{c}}\boldsymbol{x}\|^2 + \eta\|\boldsymbol{x}\|_1 \tag{5}$$

where the l_1-norm $\|\boldsymbol{x}\|_1$ promotes sparsity, the l_2-norm $\|\boldsymbol{y}_{\mathrm{c}} - \boldsymbol{A}_{\mathrm{c}}\boldsymbol{x}\|$ minimizes the errors, and a regularization parameter η balances between the two tasks. The parameter η is closely related to the detection threshold (e.g. [11]). An underdetermined system can be solved, $M < N$, because of the sparsity, i.e. only K nonzeros in $\boldsymbol{x}$ (representing the unknown $\boldsymbol{s}$), $K < M < N$, and because of the incoherence of $\boldsymbol{A}_{\mathrm{c}}$ (e.g. [1]). The mutual coherence $\kappa(\boldsymbol{A})$ of a matrix $\boldsymbol{A}$ is an incoherence measure, $\kappa(\boldsymbol{A}) = \max_{i,j,i\neq j} |\boldsymbol{a}_i^{\mathrm{H}}\boldsymbol{a}_j| / \|\boldsymbol{a}_i\| \|\boldsymbol{a}_j\|$ where $\boldsymbol{a}_n$ is the nth column of $\boldsymbol{A}$, $n = 1, .., N$. Main CS applies if $K < 1 + 1/\kappa(\boldsymbol{A})$ and $M > (K/4)\log(N/K)$ (e.g. [1]).

3. PERFORMANCE ANALYSIS

The ultimate goal of CS is to produce a CS sensor which can be simpler and still can perform at least as good as, or preferably even better, than existing sensors. Hence, we measure the performance of the four different data acquisition schemes from (2)-(4) by the SNR they can give at the output with the same signal s at the input, and receiver noise from $CN(\boldsymbol{0}, \gamma \boldsymbol{I})$ in (2)-(4) with the same variance γ.

The output SNR is measured after matched filtering (MF) of the acquired data $\boldsymbol{y}$, $\boldsymbol{y}_c$ or $\boldsymbol{y}_{\mathrm{rm}}$ from (2) to (4) because MF gives the optimal SNR and moreover, it is also the basis of SSP (as well as existing SP, e.g. [11]-[12]). The MF output $s_{c,\mathrm{MF}}$ with $\boldsymbol{y}_c$ from (3) is given by: $s_{c,\mathrm{MF}} = \boldsymbol{a}_{\boldsymbol{c}}^{\mathrm{H}}\boldsymbol{y}_c = \boldsymbol{a}_{\boldsymbol{c}}^{\mathrm{H}}\boldsymbol{a}_c s + \boldsymbol{a}_{\boldsymbol{c}}^{\mathrm{H}}\boldsymbol{z}_c$. Thus, the signal energy S_c and the noise energy N_c equal the expected values of $|\boldsymbol{a}_{\boldsymbol{c}}^{\mathrm{H}}\boldsymbol{a}_c s|^2$ and of $|\boldsymbol{a}_{\boldsymbol{c}}^{\mathrm{H}}\boldsymbol{z}_c|^2$, $S_c = E[|\boldsymbol{a}_{\boldsymbol{c}}^{\mathrm{H}}\boldsymbol{a}_c s|^2]$ and $N_c = E[|\boldsymbol{a}_{\boldsymbol{c}}^{\mathrm{H}}\boldsymbol{z}_c|^2]$, respectively.

In the reference case, $S_{\mathrm{ns}} = E[|\boldsymbol{a}^{\mathrm{H}}\boldsymbol{a}s|^2] = \|\boldsymbol{a}\|^4|s|^2 = N^2|s|^2$ and $N_{\mathrm{ns}} = E[|\boldsymbol{a}^{\mathrm{H}}\boldsymbol{z}|^2] = D[\boldsymbol{a}^{\mathrm{H}}\boldsymbol{z}] = \|\boldsymbol{a}\|^2 D[z_n] = N\gamma$, $n = 1, .., N$, where $D[\,]$ indicates the variance (dispersion).

The SS scheme is equivalent to the NS case except that the number of measurements is M in SS instead of N in NS. Thus, $S_{\mathrm{ss}} = E[|\boldsymbol{a}^{\mathrm{H}}\boldsymbol{B}_{\mathrm{ss}}^{\mathrm{H}}\boldsymbol{B}_{\mathrm{ss}}\boldsymbol{a}s|^2] = \|\boldsymbol{B}_{\mathrm{ss}}\boldsymbol{a}\|^4|s|^2 = M^2|s|^2$ and $N_{\mathrm{ss}} = E[|\boldsymbol{a}_{\mathrm{ss}}^{\mathrm{H}}\boldsymbol{z}_{\mathrm{ss}}|^2] = D[\boldsymbol{a}_{\mathrm{ss}}^{\mathrm{H}}\boldsymbol{z}_{\mathrm{ss}}] = D[\boldsymbol{a}^{\mathrm{H}}\boldsymbol{B}_{\mathrm{ss}}^{\mathrm{H}}\boldsymbol{z}_{\mathrm{ss}}] = \|\boldsymbol{B}_{\mathrm{ss}}\boldsymbol{a}\|^2 D[z_{\mathrm{ss},m}] = M\gamma$, $m = 1, .., M$.

In the AIC and RM cases, the MF signal equals $\|\boldsymbol{B}\boldsymbol{a}\|^2 s$ and becomes random due to the matrix $\boldsymbol{B}$ whose mn–th element equals $\exp(j\varphi_{mn})/\sqrt{M}$, $\varphi_{mn} \sim U(0, 2\pi)$, and whose column norm is one. Accordingly, $S_{\mathrm{aic}} = S_{\mathrm{rm}} = |s|^2 E[\|\boldsymbol{B}\boldsymbol{a}\|^4] = N^2|s|^2[1 + (N-1)/NM]$ (Appendix).

In all the sub-Nyquist schemes except SS, the noise after MF is not Gaussian anymore as it is a product involving the uniform compression $\boldsymbol{B}$ and the Gaussian noise $\boldsymbol{z}$ or $\boldsymbol{z}_{\mathrm{rm}}$.

The RM noise after MF equals $\boldsymbol{a}^{\mathrm{H}}\boldsymbol{B}^{\mathrm{H}}\boldsymbol{z}_{\mathrm{rm}}$ with the energy given by: $N_{\mathrm{rm}} = E[|\boldsymbol{a}^{\mathrm{H}}\boldsymbol{B}^{\mathrm{H}}\boldsymbol{z}_{\mathrm{rm}}|^2] = N\gamma$ (Appendix).

The AIC noise equals $\boldsymbol{a}^{\mathrm{H}}\boldsymbol{B}^{\mathrm{H}}\boldsymbol{z}$ with the energy given by: $N_{\mathrm{aic}} = E[|\boldsymbol{a}^{\mathrm{H}}\boldsymbol{B}^{\mathrm{H}}\boldsymbol{B}\boldsymbol{z}|^2] = N\gamma[1 + (N-1)/M]$ (Appendix).

Thus, the SNRs in the reference Nyquist case from (2) and the three typical compressive (sub-Nyquist) acquisition schemes from (3) and (4), can be written as follows:

$$\mathrm{SNR_{ns}} = \frac{E\left[\left|\boldsymbol{a}^{\mathrm{H}}\boldsymbol{a}s\right|^2\right]}{E\left[\left|\boldsymbol{a}^{\mathrm{H}}\boldsymbol{z}\right|^2\right]} = \frac{N^2|s|^2}{N\gamma} = N\frac{|s|^2}{\gamma} \quad (5)$$

$$\mathrm{SNR_{ss}} = \frac{E\left[\left|\boldsymbol{a}_{ss}^{\mathrm{H}}\boldsymbol{a}_{ss}s\right|^2\right]}{E\left[\left|\boldsymbol{a}_{ss}^{\mathrm{H}}\boldsymbol{z}_{ss}\right|^2\right]} = \frac{E\left[\left|\boldsymbol{a}^{\mathrm{H}}\boldsymbol{B}_{ss}^{\mathrm{H}}\boldsymbol{B}_{ss}\boldsymbol{a}s\right|^2\right]}{E\left[\left|\boldsymbol{a}^{\mathrm{H}}\boldsymbol{B}_{ss}^{\mathrm{H}}\boldsymbol{B}_{ss}\boldsymbol{z}\right|^2\right]} = M\frac{|s|^2}{\gamma} \quad (6)$$

$$\mathrm{SNR_{aic}} = \frac{E\left[\left|\boldsymbol{a}_{\mathrm{aic}}^{\mathrm{H}}\boldsymbol{a}_{\mathrm{aic}}s\right|^2\right]}{E\left[\left|\boldsymbol{a}_{\mathrm{aic}}^{\mathrm{H}}\boldsymbol{z}_{\mathrm{aic}}\right|^2\right]} = \frac{E\left[\left|\boldsymbol{a}^{\mathrm{H}}\boldsymbol{B}_{\mathrm{aic}}^{\mathrm{H}}\boldsymbol{B}_{\mathrm{aic}}\boldsymbol{a}s\right|^2\right]}{E\left[\left|\boldsymbol{a}^{\mathrm{H}}\boldsymbol{B}_{\mathrm{aic}}^{\mathrm{H}}\boldsymbol{B}_{\mathrm{aic}}\boldsymbol{z}\right|^2\right]} =$$

$$= M\left(\frac{1}{M} + \frac{N-1}{M+N-1}\right)\frac{|s|^2}{\gamma} \quad (7)$$

$$\mathrm{SNR_{rm}} = \frac{E\left[\left|\boldsymbol{a}_{\mathrm{rm}}^{\mathrm{H}}\boldsymbol{a}_{\mathrm{rm}}s\right|^2\right]}{E\left[\left|\boldsymbol{a}_{\mathrm{rm}}^{\mathrm{H}}\boldsymbol{z}_{\mathrm{rm}}\right|^2\right]} = \frac{E\left[\left|\boldsymbol{a}^{\mathrm{H}}\boldsymbol{B}_{\mathrm{rm}}^{\mathrm{H}}\boldsymbol{B}_{\mathrm{rm}}\boldsymbol{a}s\right|^2\right]}{E\left[\left|\boldsymbol{a}^{\mathrm{H}}\boldsymbol{B}_{\mathrm{rm}}^{\mathrm{H}}\boldsymbol{B}_{\mathrm{ss}}\boldsymbol{z}\right|^2\right]} =$$

$$= N\left(1 + \frac{N-1}{MN}\right)\frac{|s|^2}{\gamma} \quad (8)$$

For clarity, the SNR results are also given in Table 1.

Table 1. SNRs per data acquisition scheme (at $|s| = \gamma = 1$)

*	NS	SS	AIC	RM
SNR_*	N	M	$M\left(\frac{1}{M}+\frac{N-1}{M+N-1}\right)$	$N\left(1+\frac{N-1}{MN}\right)$
S_*	N^2	M^2	$N^2\left(1+\frac{N-1}{MN}\right)$	$N^2\left(1+\frac{N-1}{MN}\right)$
N_*	N	M	$N\left(1+\frac{N-1}{M}\right)$	N

4. NUMERICAL EXPERIMENTS

The SNR analysis is supported with numerical experiments from angle processing with antenna-array measurements. Accordingly, in the reference data model from (2), the sensing vector $\boldsymbol{a}$ is a steering vector at angle θ whose n-th element equals: $a_n = \exp(j\beta_n \sin\theta)$ where β_n is an observation variable at the n-th element (Nyquist-sampled) position. The total number N of antenna elements is chosen to be 100 while a number M of compressive measurements is chosen to be 50, 25, 20 and 10, i.e. the compression factor N/M equals 2, 4, 5 and 10, respectively. The true angle θ is chosen to be zero. The mn–th element: $\exp(j\varphi_{mn})$, of the random matrix $\boldsymbol{B}$, $\boldsymbol{B} = \boldsymbol{B}_{\mathrm{rm}} = \boldsymbol{B}_{\mathrm{aic}}$, represents a phase shift by a uniformly-distributed angle φ_{mn}, $\varphi_{mn} \sim U(0,2\pi)$. A multi-coset pattern is chosen for $\boldsymbol{B}_{\mathrm{ss}}$ and moreover, the edge elements are always kept equal to one (so that the aperture remains the same in all the acquisition schemes).

The true signal value s is chosen to be one. The noise variance γ also equals one, so that the input SNR equals one too, $|s|^2/\gamma = 1$. The output SNRs from (5) to (8) are computed numerically as the ratios of the mean values of the signal and noise energy from 1000 Monte-Carlo realizations of the noise $\boldsymbol{z}$, and of the compression matrices $\boldsymbol{B}_{\mathrm{ss}}$ and $\boldsymbol{B}$.

In Fig.1, analytical and numerical results of the SNR are compared. The results on the expected SNR coincide. Moreover, the results from RM are superior as the RM scheme holds the SNR of the Nyquist-sampled scheme but with less measurements. This is due to the CS consequence that the signal energy is preserved, i.e. $N^2|s|^2[1 + (N-1)/NM]$ w.r.t. the reference $N^2|s|^2$, while the noise energy remains the same: $N\gamma$, as given in Table 1.

In other compressive data acquisition schemes the output SNR is clearly lower depending on the compression factor N/M. In AIC the signal is preserved but the noise is stronger. In SS both signal and noise are weaker w.r.t. NS. With smaller compression factors, SS gives higher SNR than AIC. Their SNRs get closer with a higher compression factor, e.g. with N/M equal to 10 in Fig.1 whose circles coincide.

In Fig. 2, the sensing incoherence from different data acquisition schemes is given by the mean of the mutual coherence $\kappa(\boldsymbol{A}_c)$ from the same Monte-Carlo runs. SS gives higher incoherence than AIC and RM. The incoherence serves as a bound on the number M of measurements needed in CS. Note that the general CS rules (e.g. [1]) of $K < 1 + 1/\kappa(\boldsymbol{A}_c)$ and $M > (K/4)\log(N/K)$ are satisfied.

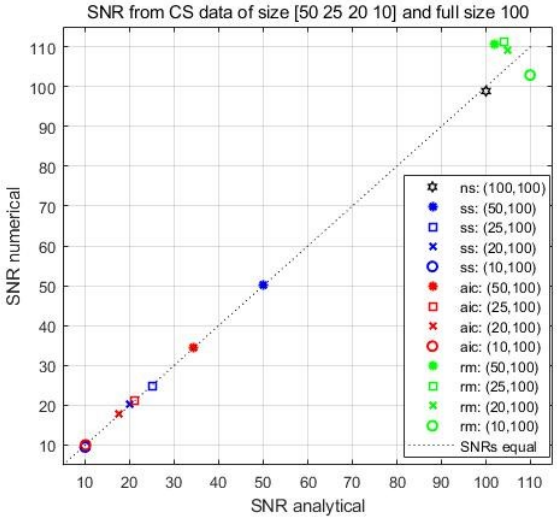

Fig. 1. SNR computed numerically from 1000 Monte-Carlo runs versus SNR from (5) to (8) of typical data acquisition schemes: Nyquist-sampled reference (ns), sparse sensing (ss), analog-to-information conversion (aic) and random mask (rm), and four compression factors: 2, 4, 5 and 10.

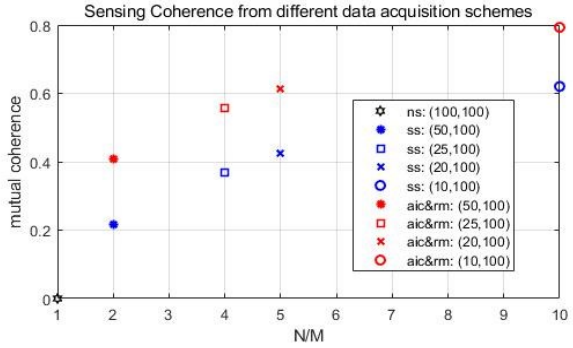

Fig. 2. Mutual coherence $\kappa(\boldsymbol{A}_c)$ from data acquisition schemes and compression factors from the same tests as in Fig. 1.

5. CONCLUSIONS

The performance of typical sub-Nyquist data acquisition schemes from CS was investigated by computing the output SNR they can provide with the same input signal. Moreover, the performance was compared with the performance of the corresponding Nyquist-sampled scheme as the reference.

The SNR analysis demonstrated that a CS sensor could be simpler with a fewer measurements and still perform as good as, if not better than, existing sensors. This is true only in the case of random-mask compressive data acquisition starting directly at reception with no receiver noise yet, and thus, affecting the signal only.

5.1. Future work

The performance of CS sensors is being further assessed by evaluating the SSP performance in detection, accuracy and resolution when random-mask compressive data acquisition schemes are applied. Furthermore, measurements and their SNRs are also being analyzed in the continuous domain to determine the reference before any sampling.

6. APPENDIX

The SNRs from (7) and (8) provided by the AIC and RM acquisition schemes, respectively, are detailed here. The SNRs are computed in the outcomes $s_{\text{aic,MF}}$ and $s_{\text{rm,MF}}$ of the matched filtering (MF) with data $\boldsymbol{y}_{\text{aic}}$ and $\boldsymbol{y}_{\text{rm}}$ from the compressive acquisition schemes AIC and RM, respectively.

The MF outputs with the AIC and RM data are given by:

$$s_{\text{aic,MF}} = \boldsymbol{a}_{\text{aic}}^{\text{H}}\boldsymbol{y}_{\text{aic}} = \boldsymbol{a}_{\text{aic}}^{\text{H}}\boldsymbol{a}_{\text{aic}}s + \boldsymbol{a}_{\text{aic}}^{\text{H}}\boldsymbol{z}_{\text{aic}} \text{ and}$$

$$s_{\text{rm,MF}} = \boldsymbol{a}_{\text{rm}}^{\text{H}}\boldsymbol{y}_{\text{rm}} = \boldsymbol{a}_{\text{rm}}^{\text{H}}\boldsymbol{a}_{\text{rm}}s + \boldsymbol{a}_{\text{rm}}^{\text{H}}\boldsymbol{z}_{\text{rm}}, \text{ respectively,}$$

where $\boldsymbol{a}_{\text{rm}} \equiv \boldsymbol{a}_{\text{aic}} = \boldsymbol{B}\boldsymbol{a}$, $\boldsymbol{z}_{\text{aic}} = \boldsymbol{B}\boldsymbol{z}$, $\boldsymbol{B}$ is a compression matrix, $\boldsymbol{B} = \boldsymbol{B}_{\text{rm}} = \boldsymbol{B}_{\text{aic}}$, $\boldsymbol{z}_{\text{rm}} \sim CN(\boldsymbol{0}, \gamma\boldsymbol{I}_M)$ and $\boldsymbol{a}$ and $\boldsymbol{z}$ as in (2). The compression matrix $\boldsymbol{B} \in \mathbb{C}^{MxN}$ contains uniformly-distributed phase shifts. Its mn–th element b_{mn} equals $\exp(j\varphi_{mn})/\sqrt{M}$ where $\varphi_{mn} \sim U(0,2\pi)$.

The signal energy after MF in AIC and RM, can be written as: $S_{\text{aic}} = S_{\text{rm}} = E[|\boldsymbol{a}^{\text{H}}\boldsymbol{B}^{\text{H}}\boldsymbol{B}\boldsymbol{a}s|^2] = |s|^2E[\|\boldsymbol{B}\boldsymbol{a}\|^4]$, where the expected value of $\|\boldsymbol{B}\boldsymbol{a}\|^4$ is further derived as: $E[\|\boldsymbol{B}\boldsymbol{a}\|^4] = D[\|\boldsymbol{B}\boldsymbol{a}\|^2] + (E[\|\boldsymbol{B}\boldsymbol{a}\|^2])^2$.

The squared norm $\|\boldsymbol{B}\boldsymbol{a}\|^2$ can be written as:

$$\|\boldsymbol{B}\boldsymbol{a}\|^2 = \sum_{m=1}^{M}|\boldsymbol{b}_m\boldsymbol{a}|^2 =$$

$$\sum_{m=1}^{M}(\sum_{n=1}^{N} b_{mn}a_n)^* (\sum_{n=1}^{N} b_{mn}a_n) =$$

$$\sum_{m=1}^{M}\sum_{n=1}^{N}\sum_{l=1}^{N}(b_{mn}a_n)^* b_{ml}a_l =$$

$$\sum_{m=1}^{M}\sum_{n=1}^{N}\{|b_{mn}|^2|a_n|^2 + \sum_{l=n+1}^{N} 2Re[(b_{mn}a_n)^* b_{ml}a_l]\}.$$

The dispersion (variance) of $\|\boldsymbol{B}\boldsymbol{a}\|^2$ can be derived as:

$$D[\|\boldsymbol{B}\boldsymbol{a}\|^2] =$$

$$\sum_{m=1}^{M}\sum_{n=1}^{N}\left\{\begin{matrix} D[|b_{mn}|^2]|a_n|^4 + \\ \sum_{l=n+1}^{N} 2Re[D[b_{mn}^* b_{ml}]|a_n^* a_l|^2] \end{matrix}\right\} =$$

$$\sum_{m=1}^{M}\sum_{n=1}^{N}\sum_{l=n+1}^{N} 2/M^2 = \sum_{m=1}^{M}\sum_{n=1}^{N} 2(N-n)/M^2 =$$

$$\sum_{m=1}^{M}(N-1)N/M^2 = (N-1)N/M.$$

where $D[b_{mn}^* b_{ml}] = E[|b_{mn}^* b_{ml}|^2] - (E[b_{mn}^* b_{ml}])^2 = 1/M^2 - 0 = 1/M^2$ and $D[|b_{mn}|^2] = 0$, and b_{mn} and b_{ml} are independent random variables with equal variances $1/M$.

Note that the computations of the dispersion or the expected value of a function $f(\varphi)$ with a uniform variable φ, $\varphi \sim U(0,2\pi)$, are based on the mean-value integral given by: $E[f(\varphi)] = \int_0^{2\pi} f(\varphi)\frac{1}{2\pi}d\varphi$. In particular, $E[\mathrm{e}^{j\varphi}] = \frac{-je^{j\varphi}}{2\pi}\Big|_0^{2\pi} = 0$, and $D[\mathrm{e}^{j\varphi}] = E\left[\left|\mathrm{e}^{j\varphi}\right|^2\right] - (E[\mathrm{e}^{j\varphi}])^2 = 1$.

The expectation of $\|\boldsymbol{B}\boldsymbol{a}\|^2$ is derived as:

$$E[\|\boldsymbol{B}\boldsymbol{a}\|^2] =$$

$$\sum_{m=1}^{M}\sum_{n=1}^{N}\{E[|b_{mn}|^2]|a_n|^2 +$$

$$\sum_{l=n+1}^{N} 2Re[E[b_{mn}^* b_{ml}]a_n^* a_l]\} = MN/M = N.$$

where $E[b_{mn}^* b_{ml}] = 0$ and $E[|b_{mn}|^2] = 1/M$.

Finally, in the AIC and RM cases, the signal energy after MF, can be written as:

$$S_{\text{aic}} = S_{\text{rm}} = |s|^2E[\|\boldsymbol{B}\boldsymbol{a}\|^4] = |s|^2[(N-1)N/M + N^2].$$

In AIC, the noise vector $\boldsymbol{z}_{\text{aic}}$ is a product of the matrix $\boldsymbol{B}$ (containing uniformly-distributed φ) with the Gaussian-distributed vector $\boldsymbol{z}$, $\boldsymbol{z}_{\text{aic}} = \boldsymbol{B}\boldsymbol{z}$. In (7) and Table 1, the noise energy N_{aic} in $s_{\text{aic,MF}}$ after MF has been derived as:

$$N_{\text{aic}} = E[|\boldsymbol{a}^{\text{H}}\boldsymbol{B}^{\text{H}}\boldsymbol{B}\boldsymbol{z}|^2] = D[\boldsymbol{a}^{\text{H}}\boldsymbol{B}^{\text{H}}\boldsymbol{B}\boldsymbol{z}] + (E[\boldsymbol{a}^{\text{H}}\boldsymbol{B}^{\text{H}}\boldsymbol{B}\boldsymbol{z}])^2 =$$

$$\sum_{n=1}^{N}|a_n|^2 D[\sum_{m=1}^{M} b_{mn}^* \sum_{l=1}^{N} b_{ml}z_n] = \cdots =$$

$$\sum_{n=1}^{N} D[\sum_{m=1}^{M}|b_{mn}|^2 z_n + \sum_{l\neq n}^{N} b_{mn}^* b_{ml}z_n] =$$

$$\sum_{n=1}^{N} D\left[\sum_{m=1}^{M}\frac{\gamma}{M} + \frac{\gamma}{M}\frac{N-1}{M}\right] = N\gamma\left(1 + \frac{N-1}{M}\right).$$

Finally, $\text{SNR}_{\text{aic}} = S_{\text{aic}}/N_{\text{aic}} = M\left(\frac{1}{M} + \frac{N-1}{M+N-1}\right)\frac{|s|^2}{\gamma}$.

In the RM scheme, the noise $\boldsymbol{z}_{\text{rm}}$ remains Gaussian, $\boldsymbol{z}_{\text{rm}} \sim CN(\boldsymbol{0}, \gamma\boldsymbol{I}_M)$. In (8) and Table 1, the noise energy N_{rm} in $s_{\text{rm,MF}}$ after MF has been derived as:

$$N_{\text{rm}} = E[|\boldsymbol{a}^{\text{H}}\boldsymbol{B}^{\text{H}}\boldsymbol{z}_{\text{rm}}|^2] = D[\boldsymbol{a}^{\text{H}}\boldsymbol{B}^{\text{H}}\boldsymbol{z}_{\text{rm}}] +$$

$$(E[\boldsymbol{a}^{\text{H}}\boldsymbol{B}^{\text{H}}\boldsymbol{z}_{\text{rm}}])^2 = \sum_{n=1}^{N}|a_n|^2 D\left[\sum_{m=1}^{M} b_{mn}^* z_{\text{rm},m}\right] = N\gamma$$

where b_{mn} and $z_{\text{rm},m}$ are independent random variables with variances $1/M$ and γ, respectively.

Finally, $\text{SNR}_{\text{rm}} = S_{\text{rm}}/N_{\text{rm}} = N\left(1 + \frac{N-1}{MN-1}\right)\frac{|s|^2}{\gamma}$.

7. REFERENCES

[1] D. Donoho, "Compressed sensing," *IEEE Trans. on IT* 52/4, 2005.

[2] J. N. Laska, S. Kirolos, M. F. Duarte, T. S. Ragheb, R. G. Baraniuk, and Y. Massoud, "*Theory and Implementation of an Analog-to-Information Converter using Random Demodulation*," Circuits and Systems, 2007. ISCAS, 2007.

[3] M. Moshe, Y. C. Eldar, and A. J. Elron, "*Xampling: Signal Acquisition and Processing in Union of Subspaces*," IEEE Transactions on Signal Processing 59.10: 4719-4734, 2011.

[4] Y. Kochman and G. W. Wornell, "*Finite Multi-coset Sampling and Sparse Arrays*," Information Theory and Applications Workshop (ITA). IEEE, 2011.

[5] M. Ibrahim, V. Ramireddy, A. Lavrenko, J. König, F. Römer, M. Landmann, M. Grossmann, G. Del Galdo and Reiner S.Thomä, *"Design and analysis of compressive antenna arrays for direction of arrival estimation",* Elsevier Signal Processing, Vol.138, pp. 35-47, September 2017.

[6] P. Pakrooh, L. L. Scharf, A. Pezeshki, and Y. Chi, "*Analysis of Fisher information and the Cramer-Rao bound for nonlinear parameter estimation after compressed sensing*", IEEE Conference ICASSP 2013.

[7] R.Pribić and G.Leus, "*Information Distances for Radar Resolution Analysis*", in Special Session on "Information Geometry in Signal Processing" at IEEE Workshop CAMSAP 2017.

[8] S. Bahmani and J. Romberg, 'Compressive Deconvolution in Random Mask Imaging', IEEE Transactions on Computational Imaging, 1.4: 236-246, December 2015.

[9] C.Tzotzadinis, "*Performance and Complexity of Data Acquisition in CS Radar*", TU Delft MSc Thesis at Thales NL, December 2017.

[10] R. Tibshirani, "Regression Shrinkage and Selection via the Lasso", J. of R. Stat. Soc, Series B, Vol. 58/issue 1, 1996.

[11] J.J. Fuchs, "The GLRT and the Sparse Representations Approach", vol. 6134, pp. 245–253, of *ICISP in Lecture Notes in Computer Science*. Springer Berlin Heidelberg, 2010.

[12] C. E. Cook and M. Bernfeld. *Radar signals; an introduction to theory and application*. Acad.Press, 1967.